GPS and Galileo Wide Area RTK concepts

Manuel Hernández-Pajares[(1)], J.Miguel Juan[(1)], Jaume Sanz[(1)], Alberto García-Rodríguez [(2)]

(1) Res. Gr. Astron. Geomatics, gAGE/UPC, Campus Nord UPC,
Jordi Girona 1, E08034-Barcelona, Spain
Contact Email: manuel@mat.upc.es
(2) ESTEC/ESA, Keplerlaan 1, Postbus 299
2200 AG, Nordwijk, The Netherlands

INTRODUCTION

The capability of providing a real-time GNSS positioning service with errors below ten centimeters at regional and continental scale strongly depend on the capability to accurately estimate the differential ionospheric corrections between GNSS receivers separated by hundreds of kilometers: The differential ionospheric refraction limits the real-time subdecimeter navigation at distances lower than 10-20 km from the nearest reference site. It impedes the carrier phase ambiguity fixing to the right integer value in the different techniques developed so far (such as RTK, LAMBDA, TCAR, FMCAR) for dual and tri-frequency receivers, for both GPS and Galileo systems. With this present state-of-the-art technique, we would need about 500 reference receivers to provide service to a mid-size country such as Spain. And several thousands would be needed to provide service to Europe. And this is unaffordable from the logistic and economic points of view. To solve this limitation, the authors started to explore, several years ago, a direct approach by providing to the users an accurate ionospheric refraction estimate to be removed from the user navigation filter equations. This was fulfilled by developing a precise technique to compute ionospheric corrections in real-time using a 3-D voxel model of the ionosphere, estimated by means of a Kalman filter, and using exclusively GNSS data gathered from fixed receivers separated several hundreds of kilometers (see Hernández-Pajares et al. 1999b, 2000a and summary of performed experiments in Hernández-Pajares et al. 2004). In this way, just few dozens of fixed reference GNSS receivers are enough to ensure a sub-decimeter positioning service at continental scale, over Europe for example. One potential network to support this service could be that which is deployed to support EGNOS, the European meter-level positioning system fulfilling integrity requirements to be used in civil aviation (see for instance Ventura-Traveset et al. 2001). The main feature of this new technique was patented for GPS dual-frequency data in 1999 (Wide Area RTK, WARTK, UPC-Patent Nbr.9902585). And the extension to three-frequency systems such as Galileo, and Modernized GPS were developed in the context of a previous project funded by ESA in 2002 (WARTK for 3 frequencies, or WARTK-3, ESA Patent Nbr.02-12627). In such new technique the ionospheric filter was combined with the TCAR algorithm (Harris 1997), allowing most part of the time an instantaneous correct fixing of ambiguities with receivers separated more than one hundred km. This was one of the main advantages of WARTK-3 in respect to WARTK-2 (or WARTK for two-frequencies systems), the potential achievement of instantaneous (at single-epoch) subdecimeter positioning at long distance (see plots at Figure 1 and details in Hernández-Pajares et al. 2002b, 2003b).

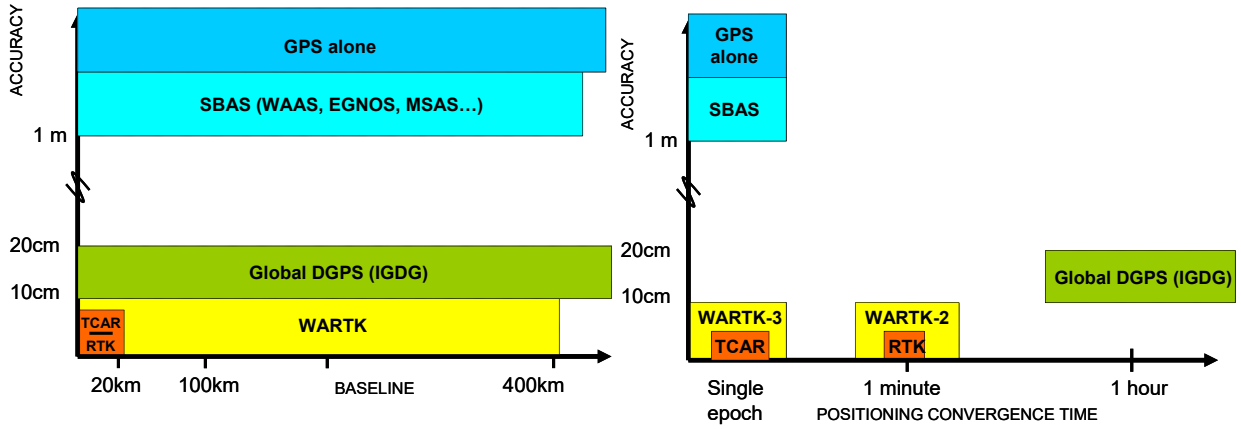

Figure 1: Accuracy versus baseline (**left-hand plot**) and Accuracy versus positioning convergence time (**right-hand plot**) for representative GNSS positioning techniques, including WARTK-2 for dual frequency signals (GPS) extending the RTK subdecimeter accuracy to baselines of hundreds of km long, and WARTK-3 for three-frequency signals (such as Galileo) providing instantaneity as well.

The main goal of this work has been the consolidation and improvement of WARTK-3 algorithm, using both actual GPS data and additional realistic three-frequency data sets, generated ad-hoc by the authors with the new Galileo signal frequency generator. Such data has served to analyze the performance of the proposed algorithm, which introduces two main improvements: (1) A new approach to maintain the integrity of the ionospheric corrections broadcasted to the users also in the presence of ionospheric perturbations, and (2) the integration of the 3 carriers ambiguity fixing in a

WARTK-3 zero-differenced (undifferenced) user navigation filter. In this way, we can take advantage of: (a) the redundance from a simultaneous real-time positioning and ambiguity estimation, and (b) the availability of new estimates to the users, among the positions, such as the orientation change ("wind-up") with a single antenna. This improved approach incorporates new capabilities regarding the previous techniques as it is depicted in Table 1.

Method	**ADVANTAGES**	**DISADVANTAGES**
TCAR	Low computational load.	Seriously limited by ionospheric refraction. Certain effect of pseudorange multipath.
ITCAR	Improved results by integrating TCAR in a navigation filter.	The ionospheric delay still limits the 3er ambiguity fixing.
FMCAR	Improved design and results by using "federated" Kalman Filters and as many carriers as available.	The ionospheric delay still limits the technique to short baselines.
WARTK (2-freq.)	Accurate real-time ionospheric modelling, allows precise navigation at hundreds of kilometers from the nearest reference site .	In spite of speeding-up the navigation Kalman filter, a significant convergence time is still needed (5-15 minutes).
WARTK-3	Uses the extra-widelane, and an accurate real-time iono. model to provide single-epoch precise navigation capabilities, and greatly speeding up the convergence of the Navigation Filter to just few epochs.	Certain effect of pseudorange multipath.
WARTK-3.2	Use of an integrated user zero-differenced navigation filter being more iono-perturbation tolerant and code multipath immune, and providing orientation change estimation to single antenna users.	

Table 1: Main advantages and disadvantages of the four real-time ambiguity resolution procedures discussed in this work: TCAR (Harris 1997), Integrated TCAR (Vollath et al. 2001), FMCAR (Vollath 2004), WARTK and WARTK-3 (Hernández-Pajares et al. 2000a and 2003b), and WARTK-3.2 (this work).

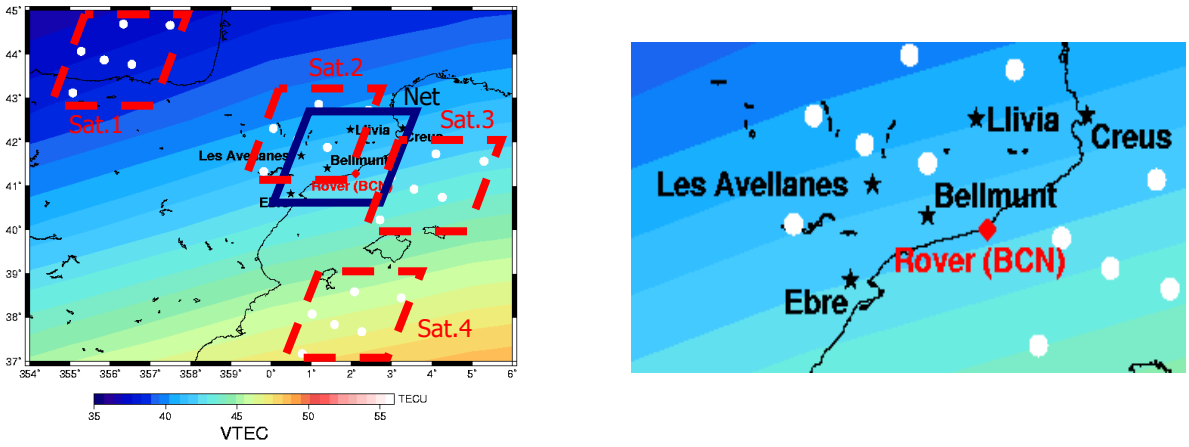

Figure 2: Regional network of the stations (dark stars) involved in the GPS experiment UNBAR01 is shown (general view, **left-hand plot**, zoom at **right-hand plot**). Such stations have been used to test the new algorithms proposed in this paper. The roving stations were placed in Barcelona, NE Spain (red diamond). The pierce points of 4 high elevation satellites in view, merged in corresponding clusters, are also indicated with white circles, as far as the TEC distribution over the region (at 13 UT approximately of day 162, 2003).

FIRST IMPROVEMENT: INTEGRITY OF THE IONOSPHERIC CORRECTIONS

One of the most difficult scenarios that sometimes appears at mid-latitudes is the presence of ionospheric waves (Traveling Ionospheric Disturbances, TIDs) in the GNSS Wide Area network. They produce a non-linear behavior of the Ionosphere, which can affect the interpolation performance of the differential ionospheric delays between the reference stations (see for example Orús et al. 2003). This interpolation capability is usually essential to provide accurate values to the roving users in the Wide Area network. One way to overcome -or at least mitigate- these problems is the use of a real-time ionospheric filter by the roving user (Hernández-Pajares et al. 2001b, 2002b). In this context we have improved the WARTK-3 and WARTK techniques, by incorporating a gradient step detector of the ionospheric differential delay in the reference stations. The performance of this approach has been studied using real GPS data gathered in Spain (see below). The results suggest a significant improvement in the problem when the gradient step detector is used. Indeed, once the unambiguous Slant Total Electron Content (STEC) is computed in the reference stations, these values can be used to provide, through an interpolation, the STEC value for any user in the coverage area. The method of interpolation will depend on the size of the area as well as the ionospheric conditions. For instance, in small networks (i.e. distances up to few hundreds of kilometers) and quiet ionospheric conditions, the

interpolated STEC value for the user can be obtained by combining the corresponding values in the reference stations with fixed weights. In this work, and for each satellite in view from the reference stations, a planar (or quadratic) adjustment is made by estimating the 2 (or 5) components of the between-station single STEC difference gradient. From this gradient (or gradient and Hessian), any user in the coverage area can compute its own single difference of STEC with respect to the reference stations for a given satellite. This is done in this way because the pierce points of the satellites in view from a regional network appear clustered differently for each satellite reproducing the geometry of the network but in different ionospheric regions, and with different gradients in general (see Figure 2). This is useful to interpolate easily to the position of the roving receivers. The main advantage of this approach is that we can include in the gradient computation additional information as ionospheric models and temporal continuity. And this allows the system to monitor the quality of this planar adjustment in the reference stations in order to detect ionospheric irregularities such as TIDs, avoiding its direct effect on the users.

SECOND IMPROVEMENT: INTEGRATION OF WARTK-3 IN A NAVIGATION FILTER (WARTK-3.2)

The user algorithm, which integrates WARTK-3 in a unique navigation filter, is represented in Figure 3 and it can be briefly described for the different components indicated in such layout:

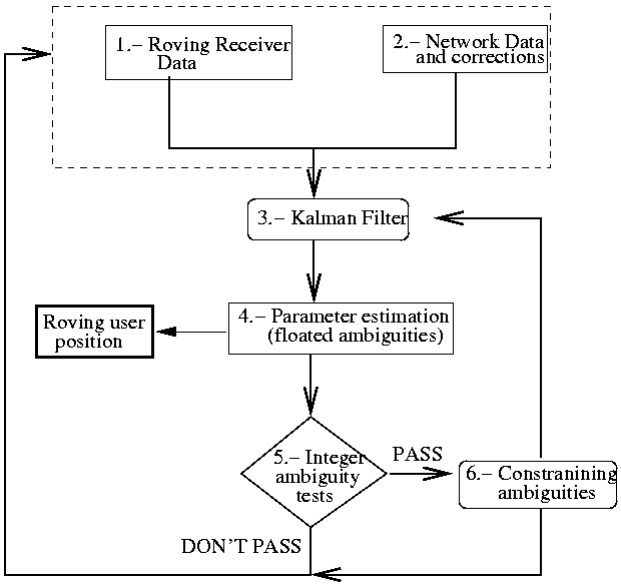

Figure 3: WARTK-3.2 algorithm layout for the roving user.

Step 1 "Roving Receiver Data": The algorithm is fed with data measured with a Galileo or Modernized GPS receiver. These data consist of 3 carrier phase measurements (L1, L2, L3) and 3 code measurements (P1, P2, P3) for each satellite in view, which are used simultaneously during each observation epoch (typically each second). As in the case of the reference stations algorithm, six combinations of these types of observations are used. These are the difference of wide lane and extra-wide lane carrier phases (L_w-L_{ew}), the ionosphere-free carrier-phase combination (L_c), the ionospheric (geometry-free) combination (L_I), the extra-wide lane carrier-phase minus pseudorange difference (L_{ew}-P_{ew}), the wide-lane carrier phase minus pseudorange difference (L_w-P_w) and the ionosphere-free pseudorange combination P_c. If the user does not choose to calculate his/her own ionospheric model (this is usually not necessary), the geometric-free observations L_I are only used to compute the ambiguity ionospheric carrier phase combination B_I from the STEC computed and provided externally.

Step 2 "Network Data and corrections": Beside the data from its own receiver, the user must receive data and differential corrections from the network of reference stations. These data are: (1) The same six combinations of measurements as in the rover but only from one reference station receiver. These measurements are necessary in order to compute satellite clocks and to fix integer values of double differenced ambiguities. And (2), the single-differenced STEC for each satellite in view is interpolated to the rover position from the surrounded reference stations STECs. These values are broadcast jointly with a parameter of quality indicating the confidence of the ionospheric correction.

Step 3 "Kalman Filter": The observable equations are approximated by a linear expansion in a rover position computed from a standard positioning technique using pseudorange data. They are solved in the framework of a forward Kalman Filter. The data from the receiver and from the network are modelled taking into account:

1) The program runs on absolute mode (without double differencing the measurements, i.e. zero-differenced). The initial disadvantage of this approach is that it implies a more complex model and it is necessary to estimate more parameters such as the wind-up, delay code biases and satellite and receiver clocks that mostly cancel out when double differences are made. The advantages, on the one hand, are that we can, and we do, estimate the parameters (such as the

wind-up, providing the rover orientation change) and on the other hand, that we can use any additional information of these parameters that would improve the estimations of the overall unknowns, in particular the real-time position.

2) Note that the estimation of the antenna orientation is only possible from the equation on the ionospheric carrier phase combination LI: although the wind-up appears on the Lc equation, it cannot be distinguished from the rover clock parameter. The reason is that the effect is essentially the same for all the satellites when the rover is moving horizontally.

3) With this procedure the satellite clocks are referred to the reference station clock. In order to maintain such values close to the GPS time, it is necessary to send the estimation of the reference station clock to the user.

Steps 4 "Parameter estimation" and 5 "Integer ambiguity tests": Once the filter provides estimations for the ambiguities, the following step is to fix double-differenced ambiguities to its integer values. Several tests are made in order to maximize the probability of fixing these ambiguities to their correct values. Such tests mainly look at the widelane ambiguity formal and round-up error, quality of transmitted differential ionospheric correction and ambiguity parity checks for GPS data. In general, the checking and fixing of ambiguities with three-frequencies are performed going from the longest to the shortest wavelength, fixing and updating the covariance each time the tests are passed.

Step 6 "Constraining ambiguities": From the integer values of L1, Lw and Lew double differenced ambiguities, the corresponding ionospheric and ionosphere-free ambiguities can be estimated and introduced as additional constraints in the Kalman filter in order to improve the parameter estimation of the next epoch.

RESULTS WITH ACTUAL GPS DATA: UNBAR01 EXPERIMENT

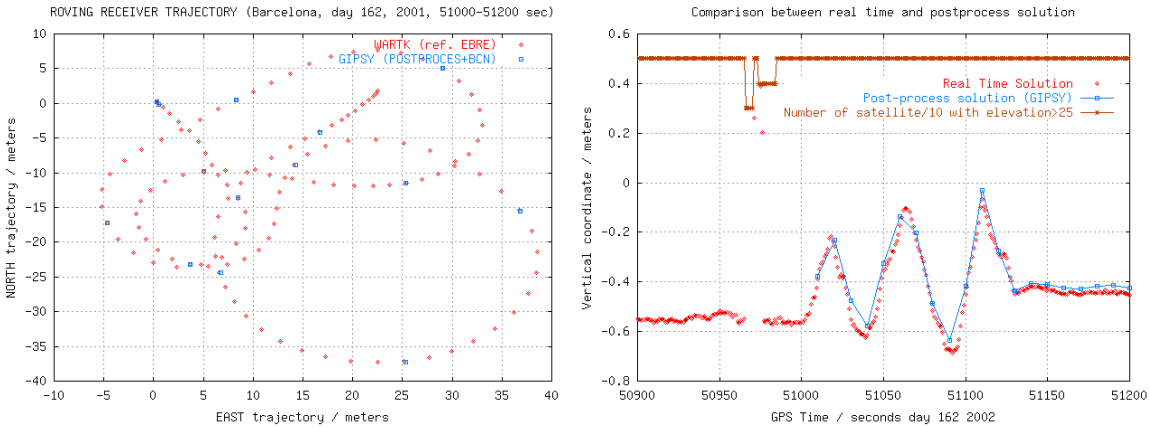

Figure 4: In the **left-hand plot** the roving car trajectory (North-East) for two minutes is shown. The red trajectory has been computed with WARTK being the closest station, Bellmunt, at 67 km away. And the reference trajectory (blue) is computed with GIPSY software (in post-process and using very close reference station data). In the **right-hand plot** the vertical component (Up) is shown. It corresponds, approximately, to the horizontal movement estimated in the left-hand plot.

In order to test the performance of the improved technique, two main datasets have been used. They consist on actual GPS measurements and signal-simulated observables in 3-frequencies. The first dataset corresponds to the GPS Urban Navigation in Barcelona, Spain – 2001 experiment (hereinafter UNBAR01) which was performed the 11th of June, 2001, coinciding with Solar Maximum conditions. Two roving receivers placed on the roof of a car at a distance of about 77.5 cm were gathering data on a trail of several km in Barcelona city. And a set of permanent receivers belonging to the Cartographical Institute of Catalonia (CATNet) was used in the computation of the differential corrections in real-time mode with the WARTK technique (see Figure 2). The difficulty of this scenario is still higher due to the presence of ionospheric waves (TIDs) and to the outer position of the roving station regarding the reference network. Thus the two potential improvements in WARTK-3 described above have been tested. The double differenced ionospheric values of the rover fit quite well below such value after substracting the interpolated ionospheric corrections from the network of stations (using the gradient detector mentioned above to filter out the existing ionospheric perturbations). The main results are summarized in Figure 5 . The trajectory of the car is compared with the post-process solution using the JPL software GIPSY (see for instance Webb and Zumberge, 1997), which used additional data coming from a very close reference station (BCN) at few kilometers away. This post-processed solution is obtained every 10 seconds. A good agreement of about few centimeters of WARTK can be seen using Bellmunt as the closest reference station, at about 70 km away. Indeed, in Figure 4 we show the horizontal (left-hand plot) and vertical results (right-hand plot) during a typical period of movement (for 120 consecutive seconds), with an agreement at the level of few centimeters. This figure illustrates the case of 3 simultaneous cycle-slips, in such a way that the positioning around the epoch 50970s must be done with only 1 fixed double difference and 4 available satellites. Some few very bad estimates have been filtered out in real-time mode as well, by means of the positioning sigma computed by the user. After these epochs, the positioning error quickly returns to just few centimeters. Finally, in Figure 9 the horizontal movement (left-hand plot) and corresponding wind-up estimated from the ionospheric measurements (right-hand plot) are represented. These results are compatible at the measurement error level of few degrees.

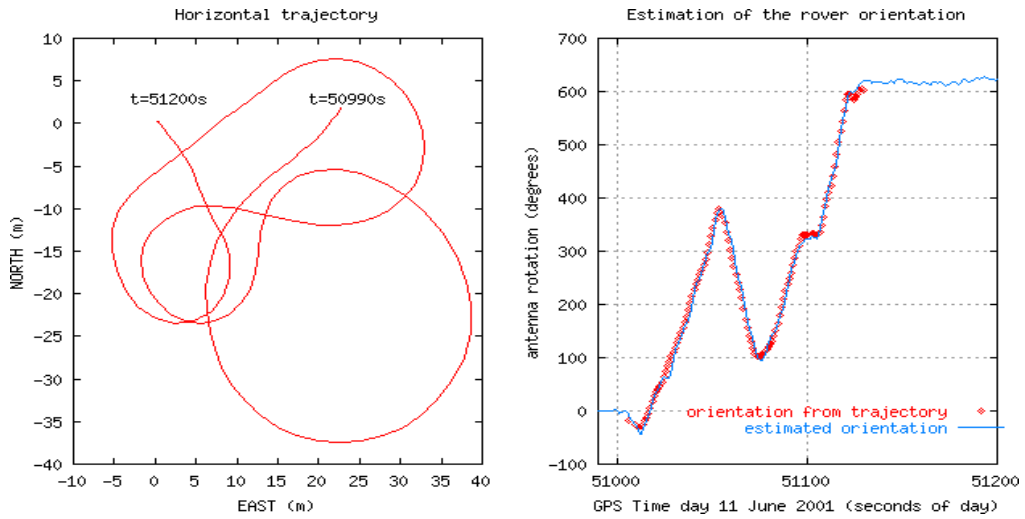

Figure 5: Plots showing the horizontal movement of the roving receiver, during a part of the UNBAR01 experiment (**left side plot**). At the **right hand plot**, the corresponding wind-up estimation (blue) is compared with the value derived from the trajectory (red).

RESULTS WITH 3-FREQUENCIES DATASETS

Several datasets were simulated in the RNEU GSVF facility (Figure 6 right-hand plot, see as well document P6908-35-011), during January 2004 at ESTEC/ESA, in the context of the present "WARTK-3 Laboratory Test Campaign" project. These datasets were used to characterize the performance of the WARTK-3.2 technique describe before. The GNSS receiver used the data gathered at frequencies corresponding to E1 (1.589742 GHz, wavelength of 18.9 cm, also called S1) and E2 (1.256244 GHz, wavelength of 23.9cm, also called S2), in conjunction with S3 (1.561098 GHz, wavelength of 19.2 cm), to be able to compute an extra-wide lane combination (see below). From the carrier phases S1, S2 and S3, and pseudoranges, P1, P2 and P3, everything in meters, the following combinations are used: (1) Ionospheric combination, S_i = S1 - S2 P_i = P2 - P1. (2) Ionospheric-free combination of S1 and S2, (3) The wide-lane combination S_w (wavelength λ_w= 0.90 m) and (4) The extra wide-lane combination (λ_e =10.47m).
The summary of the results obtained applying the improved WARTK3.2 technique is mainly shown in a representative scenario (a): surface rover (ROVE) navigating at 178 km from the nearest reference station (NRS). The results corresponding to the other two analyzed scenarios ((b) air rover (AIR1) navigating at 238 km from the NRS, and (c) fixed receiver (MADR) navigated as real rover, at 404 km away from the NRS) are only briefly commented (see details in Hernández-Pajares et al. 2004). The WARTK-3 resulting performance of the real-time ionospheric corrections provided to the user and the corresponding real-time positioning will be detailed in the worst case scenario under Solar-Maximum Ionosphere conditions. The error in GPS orbit is not simulated because its value can be typically removed at the cm-level or better, by adjusting the orbits with the permanent network data and/or using predicted accurate orbits.

Scenario (a): Surface roving receiver (ROVE) results

In this scenario one surface rover receiver (ROVE) was simulated, navigating in Catalonia at the NE part of Spain. The closest reference receiver used was CREU, at 178 km away (see Figure 6) being the additional fixed stations used TOUL, PALM, MADR, SADC, LISB and MALA), and the worst case ionospheric scenario under Solar Maximum conditions was considered. The first point which performance has been analyzed is the error of the real-time ionospheric corrections provided to the user (or interpolation problem). The International Reference Ionosphere model (IRI, Bilitza 1990) has been used to simulate the ionospheric delays. Such model predicts realistic ionospheric refraction values, but without considering ionospheric waves (Traveling Ionospheric Disturbances, TIDs), which were covered in the integrity study performed above. Moreover, we have concentrated our study on the ionospheric interpolation problem, by considering that the carrier phase ambiguities between the reference permanent GNSS stations can be fixed correctly in real-time (this has been proven with actual GPS data up to baselines of thousands of kilometers, see Hernández-Pajares et al. 2002a).

One important result obtained in this scenario is that with the corresponding high ionospheric values, a planar fit (commented above in "Gradient method description") is not accurate enough for the interpolation task. However a 2nd order (quadratic) interpolation procedure of the between-stations single differences is accurate enough to guarantee the achievement of errors below the exigent limit of 2.5 cm of the ionospheric combination, S1-S2=S_i. This is due to the high values and variations achieved by the ionospheric refraction in the Solar Maximum scenario and, the sometimes strong ionospheric slant TEC variation of the rays coming from the South and crossing tails of the Equatorial Anomalies. Indeed, in this scenario, the user ionospheric interpolation error decreases when we pass from using planar fit (below 7cm) to using quadratic interpolation (below 2cm). In this way, with the quadratic interpolation, 100% of

real-time interpolated double-differenced STEC at ROVE are below the threshold value of 2.5cm of Si ($[\lambda_2-\lambda_1]/2$, see Hernández-Pajares et al. 2000a.), with an RMS of 0.5 cm. As was proposed in the first part of this study, the user will apply the ionospheric corrections received from the fixed stations network in the framework of a general navigation Kalman filter feed with zero-differenced (undifferenced) observations. With 3-frequencies measurements 100% of ambiguities are fixed since the beginning and the real-time positioning error decrease below 10 cm after a convergence time of just few seconds, needed to decorrelate the tropospheric delay (the navigation has been started at 47100 sec, coinciding with the simulator availability of common satellites: see Figure 7, left-hand plot).

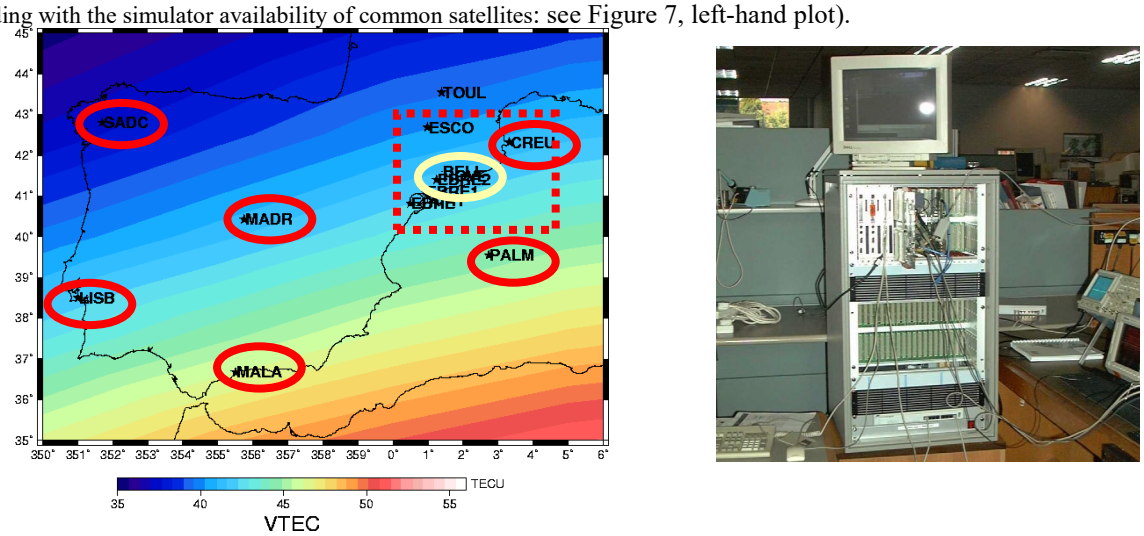

Figure 6: In the **left-hand plot** the Scenario layout is depicted (yellow ellipse=rover, red ellipse=fixed stations). In the **right-hand plot** the Galileo Signal Simulation Facility is shown (ESTEC/ESA, Nordwijk, The Netherlands, GSVF, courtesy of Thales).

The results are practically equivalent in single epoch mode (with an RMS of 1.4 cm) emulated as a continuous cold start (setting up all the variances to ∞), but maintaining the random walk tropospheric estimation. We have studied as well the corresponding performance with 2-frequencies systems in order to compare with 3-frequencies systems. Indeed, when we simulate a cold starting-up with two-frequencies data, we get as well a sub-decimeter real-time positioning such as with three-frequencies (RMS of 2 cm and 100% amb. fixed), but after a convergence time of approximately 100 sec (time needed for both ambiguity fixing and initial tropospheric state estimation), instead of instantaneously (Figure 7). This result is in concordance with that obtained with actual GPS data. The corresponding positioning errors for ROVE moving around the scenario (a) are lower than 6 cm, obtaining a RMS of 2,4 cm (3-D), with an RMS of 1.7, 0.4 and 1.5 cm in X,Y,Z components, respectively. As it was commented above WARTK-3.2 provides, simultaneously to the rover position, an estimate of the antenna orientation change (wind-up) by comparing its own ambiguous undifferenced STEC with the external ionospheric correction gathered from the network. It can be seen in Figure 8 that the single rover antenna orientation change (wind-up) is estimated in real-time with an RMS of 4.8 degrees being the corresponding maneuvers plotted in the same figure (the offset is meaningful because it corresponds to an arbitrarily initial reference orientation).

Scenario (b): Airplane roving receiver (AIR1) results

In order to show the performance of WARTK-3.2 used with GNSS receivers under high dynamics, we have analyzed the scenario (b) corresponding to an airplane describing several turns in the same region (Catalonia at NE Spain) as the surface rover, close to EBRE, which has not used in the computations (see Figure 6, left hand plot). In this case, the nearest reference receiver (PALM) is located at about 238 km away from the airplane which flies again in the worst case of the ionospheric scenario under Solar Maximum conditions. For the airplane AIR1, the effect of the high dynamics of the receiver produces important non-linear variations of the differential ionospheric values. In spite of this wave-like variation, the 100% of real-time interpolated differential STECs at AIR1 is below the threshold value of 2.5 cm (RMS of 0.5 cm). One of the points in the accurate real-time positioning of airplanes is the high rate of height change producing high variations of tropospheric delay, converting its accurate estimation in an issue that can affect seriously the navigation quality. This point is clear in Figure 9, where WARTK-3.2 with the standard permanent receiver random process noise for the vertical tropospheric delay produces a significant error in periods with strong height changes of the airplane (such as 48100-48200 sec). The accuracy improves significantly (sub-decimeter values) when more freedom (higher random process noise) is applied to the troposphere, both in navigation filter and single-epoch modes (see again Figure 9).

Scenario (c): Long distance results (MADR)

A third scenario has been studied in order to characterize the performance of WARTK-3.2, in particular the accurate interpolation of ionospheric corrections, at still longer distances and maintaining the Solar Maximum ionospheric

conditions. In this scenario MADR, fixed station treated as rover is located at 404 km away from EBRE, the nearest fixed site (see Figure 6). In spite of the long distance and Solar-Maximum scenario, 98.7% of real-time interpolated double-differenced STEC at MADR is below the threshold value of 2.5cm of Si (RMS value of 0.8 cm), and the corresponding navigation with an error below few centimeters is achieved.

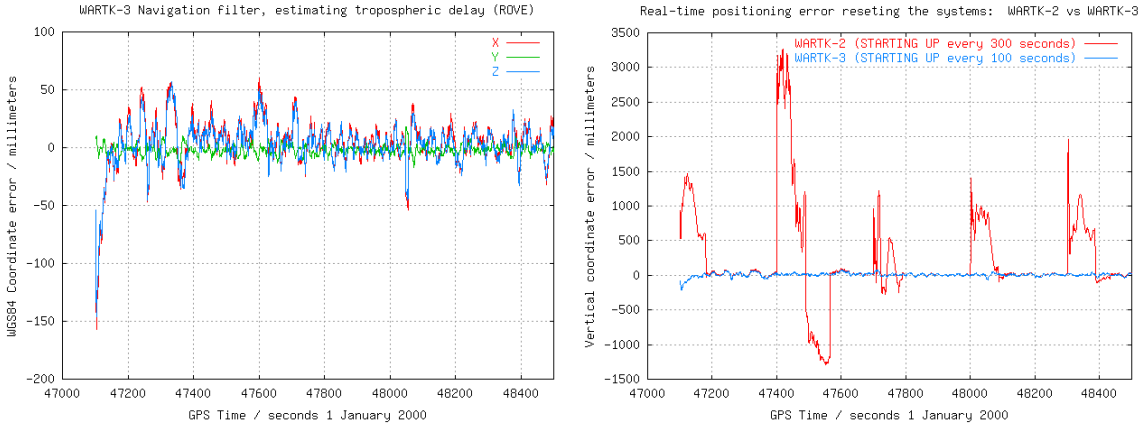

Figure 7: Left-hand plot: ROVE WARTK3 Navigation: X,Y,Z errors (scen. a). **Right-hand plot**: WARTK3.2 vs WARTK-2 WGS84 Vertical (up) positioning error for ROVE in scenario (a), starting up everything each 100/300 sec. respectively (including tropo.).

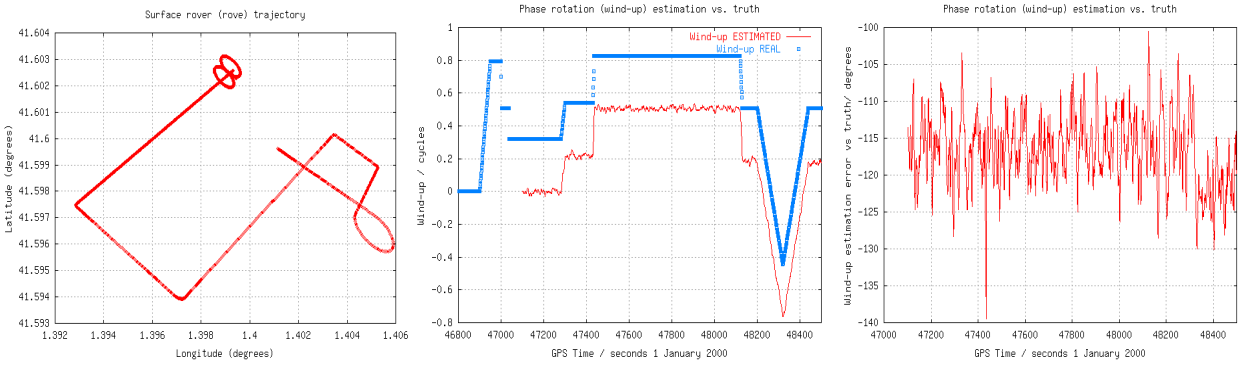

Figure 8: Left-hand plot: Horizontal projection of the ROVE trajectory, which is reflected in the wind-up values to be estimated. **Central plot**: Real-time phase orientation change estimation (wind-up) in ROVE (red) vs. the real one (blue). **Right-hand plot**: corresponding errors (including an arbitrarily initial orientation value) of the antenna rotation instantaneous estimation.

Summary of different results

Worst case scenarios for the real-time filter and single-epoch navigation have been also considered, including high tropospheric variation and high multipath with extreme measurement noise. RMSs of 2 and 0.5 cm for vertical and horizontal positioning are attained for both real-time navigation filter and single-epoch mode after an initial period of about 20 seconds to estimate the initial tropospheric state in such nominal case. In the case of the navigation filter the worst results are obtained with high tropospheric variation in the airplane scenario (RMSs of 4 and 3 cm in vertical and horizontal components).

CONCLUSIONS

An improved approach of Wide Area Real Time Kinematics (WARTK) with 2 and 3 GNSS frequencies has been presented, including the design and testing with real GPS data and simulated GALILEO signals. The inclusions of a gradient step detection approach, and the integration of the WARTK-3 algorithm in a user navigation filter scheme – which include some novel approaches such as the simultaneous user orientation parameters for one single antenna- are two new features among others of WARTK-3.2. The good performance of WARTK-3.2 has been shown firstly with GPS data (WARTK-2), and in a difficult scenario from both points of views: the ionosphere (Solar Maximum and local perturbations) and the navigation in an urban scenario, at the outer part of the network. The improved technique WARTK-3.2 has been tested as well with 3-frequencies datasets generated by the authors in the new Galileo signal generator, within Solar Maximum conditions at mid latitude, in three scenarios: car, airplane and fixed station treated as rovers, at 178, 238 and 404 km away from the corresponding nearest reference site. Another new result summarized in this work is the real-time orientation change performed at the level of 5 degrees of RMS by the roving user with a single antenna thanks to the ionospheric broadcasted corrections and the zero-differenced approach to solve the navigation state. The results confirm previous studies: WARTK3.2 makes a new navigation service feasible with errors of few centimeters from national and continental networks of GNSS stations separated by hundreds of km. This accurate real-time positioning can be typically achieved instantaneously with 3-frequency systems (such as Galileo and Modernized

GPS). With the current GPS the accurate (centimeter error level) can be obtained in real-time, but after the best part of 1-2 minutes during a receiver cold start. The results obtained so far suggest the maturity of the WARTK technique in order to built a first prototype based on the EGNOS (or other SBAS systems) RIMS data stream, gathered through Internet (SiSNET/INSPIRE, Torán-Martí and Ventura-Traveset, 2004).

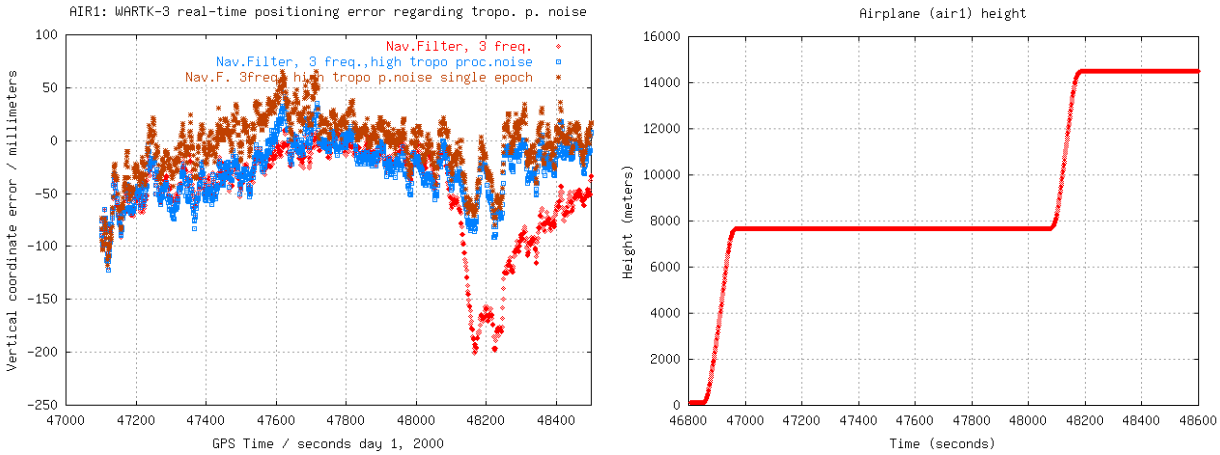

Figure 9: Left-hand plot: WARTK-3.2 Vertical coordinate error compared between using a standard ground-based tropospheric random-walk process noise (red), and using a higher process noise (blue and brown in single-epoch mode as well). The improvement is clear during the high increase of height (**right-hand plot**).

ACKNOWLEDGMENTS

The authors of this report are grateful to the Cartographical Institute of Catalonia (ICC) and to the International GPS Service (IGS), to make publicly available several GPS datasets used in this work. This work has been performed under ESA/ESTEC Contract Number 15453/01/NL/LvN-CCN01, being Alberto García-Rodríguez the contractor manager.

REFERENCES

Billitza D., International Reference Ionosphere 1990, URSI/COSPAR, NSSDC/WDC-A-R&S 90-22, 1990.

Colombo O., Hernández-Pajares M., Juan J.M., Sanz J., J. Talaya, Resolving carrier-phase ambiguities on-the-fly, at more than 100Km from the nearest reference, with the help of ionospheric tomography, Awarded oral presentation, Institute of Navigation GPS'99, Nashville (USA), 1999.

Colombo O., Hernández-Pajares M., Juan J.M., Sanz J., Ionospheric tomography helps resolve GPS ambiguities On The Fly at distances of hundreds of kilometers during increased geomagnetic activity, PLANS 2000, San Diego, USA, 2000.

Colombo O., Hernández-Pajares M., J.M. Juan, J. Sanz, Wide-Area, carrier-phase ambiguity resolution using a tomographic model of the Ionosphere, Navigation, 49(1) p. 61-69, 2002.

Harris, R.A.: Direct Resolution of Carrier-Phase Ambiguity by 'Bridging the Wavelength Gap', ESA Publication "TST/60107/RAH/Word", 2/1997.

Hernández-Pajares M., J.M. Juan, J. Sanz and O.L. Colombo, Precise ionospheric determination and its application to real-time GPS ambiguity resolution, Institute of Navigation ION GPS'99, Nashville, Tennessee, USA, September 1999b.

Hernández-Pajares, M., J.M. Juan, J. Sanz and O.L. Colombo, Application of ionospheric tomography to real-time GPS carrier-phase ambiguities resolution, at scales of 400-1000 km, and with high geomagnetic activity, Geophysical Research Letters, 27, 2009-2012, 2000a.

Hernández-Pajares M., Juan J.M., Sanz J., O. Colombo, H. Van der Marel, Precise ionospheric determination and its application to real-time GPS ambiguity resolution, Institute of Navigation ION-GPS'2000, Salt-Lake, USA, 2000b.

Hernández-Pajares M., J.M. Juan, J. Sanz, O. Colombo, and H. van der Marel, A new strategy for real-time integrated water vapor determination in WADGPS networks, Geophysical Research Letters, 28 No.17 p. 3267-3270, 2001a.

Hernández-Pajares, M., J.M. Juan, J. Sanz, O.L. Colombo, Tomographic modeling of GNSS ionospheric corrections: Assessment and real-time applications, ION GPS'2001, Salt Lake, USA, September 2001b.

Hernández-Pajares M., J.M. Juan, J. Sanz and O. Colombo, Improving the real-time ionospheric determination from GPS sites at Very Long Distances over the Equator, Journal of Geophysical Research - Space Physics, (A) Vol. 107, pp.1296-1305, 2002a.

Hernández-Pajares, M., J.M. Juan, J.Sanz, Wide Real Time Kinematics with three-carrier phases (WARTK-3), Final Report, ESA/ESTEC Contract Number 15453/01/NL/LvH, Technical Manager: Alberto García-Rodríguez, September 2002b.

Hernández-Pajares, M., J.M. Juan, J.Sanz, O.L.Colombo, Feasibility of Wide-Area Subdecimeter Navigation With GALILEO and Modernized GPS, IEEE Transactions on Geoscience and Remote Sensing, Vol.41, No.9, September 2003a.

Hernández-Pajares M., Juan J.M., Sanz J., O. Colombo, Impact of Real-Time Ionospheric Determination on Improving Precise Navigation with GALILEO and Next-Generation GPS, NAVIGATION: Journal of The Institute of Navigation, Vol.50, No.3, pp.205-218, Fall 2003b.

Hernández-Pajares, M., J.M. Juan, J.Sanz, A.García-Rodríguez, O.L.Colombo, Wide Area Real Kinematics with Galileo and GPS Signals, Awarded Best Presentation at ION-GNSS 2004, Long Beach, CA, USA, September 2004.

Orús, R., M. Hernández-Pajares., J.M. Juan, J.Sanz, Ionospheric Effects on Precise Navigation at Regional and Continental Scales over Europe, ISPRS International Workshop "Theory, Technology and Realities of Inertial / GPS Sensor Orientation", Castelldefels, Spain, 22-23 September 2003.

Teunissen, P. J., C. C. De Jonge, J.M. Tiberius, Performance of the Lambda method for fast GPS ambiguity resolution, Navigation 44(3), 1997.

Torán-Martí F. and J. Ventura-Traveset, The ESA SISNeT Project: Current Status and Future Plans, European Navigation Conference GNSS 2004.

Ventura-Traveset J., P. Michel, L. Gauthier, Architecture, Mission and Signal Processing Aspects of the EGNOS System: the first European Implementation of GNSS, Seventh International Workshop on Digital Signal Processing Techniques for Space Communications, DSP 2001, Sesimbra, Portugal, 1-3 October 2001.

Vollath, U., E. Roy, Ambiguity Resolution using Three Carriers -Performance Analysis using "Real" Data, GNSS Symposium, Seville, May 2001.

Vollath, U., TCAR Test-2 Final Presentation, GNSS Final Presentations Days, ESTEC/ESA, Nordwijk, April 2004

Webb F.H and J.F. Zumberge, An introduction to GIPSY/OASIS-II, JPL D-11088, 1997.

P6908-35-011-Issue3: GNSS-2 Signal Validation, Receiver to NPU Interface Control Document, Thales Navigation, ESA Contract No. RR029281, 6 November 2001.